Soft Matter

PAPER

View Article Online
View Journal | View Issue

Cite this: *Soft Matter*, 2026, **22**, 518

Resolving toughness-modulus conflict in carbon black reinforced natural rubber by preserving long chains†

Chenghai Li,‡[a] Matthew Wei Ming Tan,‡[ab] Xianyang Bao,[a] Guodong Nian,[a] Yakov Kutsovsky[c] and Zhigang Suo*[a]

Received 27th September 2025,
Accepted 1st December 2025

DOI: 10.1039/d5sm00983a

rsc.li/soft-matter-journal

In manufacturing many natural rubber products, carbon particles and natural rubber chains are mixed by high-intensity processes, such as roll milling and internal mixing. These processes cut natural rubber chains and reduce the performance of the composite. Here we hypothesize that the performance can be enhanced by preserving long chains of natural rubber. We test this hypothesis by mixing carbon particles with natural rubber latex without cutting chains. The long chains are densely entangled and sparsely crosslinked. Above a certain volume fraction, carbon particles percolate. The percolated network of carbon particles and the crosslinked network of rubber chains interpenetrate and form strong noncovalent bonds. Preserving long chains amplifies toughness by more than an order of magnitude, from $\sim$3.5 kJ m^{-2} to $\sim$63 kJ m^{-2}, while maintaining modulus. High toughness arises from energy dissipation across multiple length scales: along long rubber strands, across carbon particles, and in a zone of strain-induced crystallization and interfacial dissipation. Modulus is maintained through entanglements of rubber strands and percolation of carbon particles.

1. Introduction

Of all rubbers, natural rubber stands out for having long chains,[1,2] low interchain friction,[3] and near-perfect stereoregularity.[4,5] The long chains lead to high strength and fatigue resistance.[6,7] The low interchain friction reduces hysteresis.[3,6,7] The near-perfect stereoregularity enables strain-induced crystallization (SIC), which amplifies toughness.[6–8] This combination of attributes has not been reproduced in synthetic rubbers.[9] The long chains of natural rubber, however, are cut short to ease manufacturing of many products.[10,11] Nature synthesizes long polymers, but humans cut them short. The long chains of natural rubber have so far benefited a few products, including condoms, gloves, and liners for mining equipment.

Applications, such as tires, hoses, and engine mounts, require high modulus to resist deformation, and high toughness to resist crack growth. Modulus and toughness often conflict in materials.[12–16] When chains are cut short, forming a polymer network requires dense crosslinks,[17] which increase modulus but decrease toughness.[18] This conflict between modulus and toughness is resolved in a class of networks, called tanglemers, in which entanglements greatly outnumber crosslinks.[19,20] In a tanglemer, dense entanglements lead to high modulus and sparse crosslinks lead to high toughness. We have recently prepared a natural rubber tanglemer without cutting long chains.[7] The natural rubber tanglemer greatly amplifies toughness while maintaining modulus. We have also recently synthesized a silica reinforced poly(ethyl acrylate) tanglemer, which achieves a high resistance to crack growth under cyclic loadings.[21] We have also demonstrated that silica reinforced natural rubber without cutting chains achieves a combination of high modulus and toughness.[22]

A widely used filler is carbon black, with global production of 12.2 million tons annually, 90% of which is used to fill both natural and synthetic rubbers.[23–27] Carbon black reinforced natural rubber outperforms carbon black reinforced synthetic rubbers and is the material of choice for high severity applications, such as tires for trucks, buses, aircrafts, and mining vehicles.[23,24,26,28] Rubber chains and carbon particles form strong noncovalent bonds, such as van der Waals interactions and π–π interactions.[23,24,26,28,29] Carbon black reinforced natural rubbers have been widely used because the addition of carbon black preserves SIC.[30–32] Prior research, however, has

[a] *John A. Paulson School of Engineering and Applied Sciences, Harvard University, MA 02138, USA. E-mail: suo@seas.harvard.edu*
[b] *School of Materials Science and Engineering, Nanyang Technological University, 50 Nanyang Avenue, Singapore 639798, Singapore*
[c] *Expert-in-Residence, Office of Technology Development, Harvard University, Cambridge, MA 02138, USA*

† This paper is submitted to the *Soft Matter* special issue to mark the 70th birthday of Michael Rubinstein.

‡ These authors contributed equally to this paper.

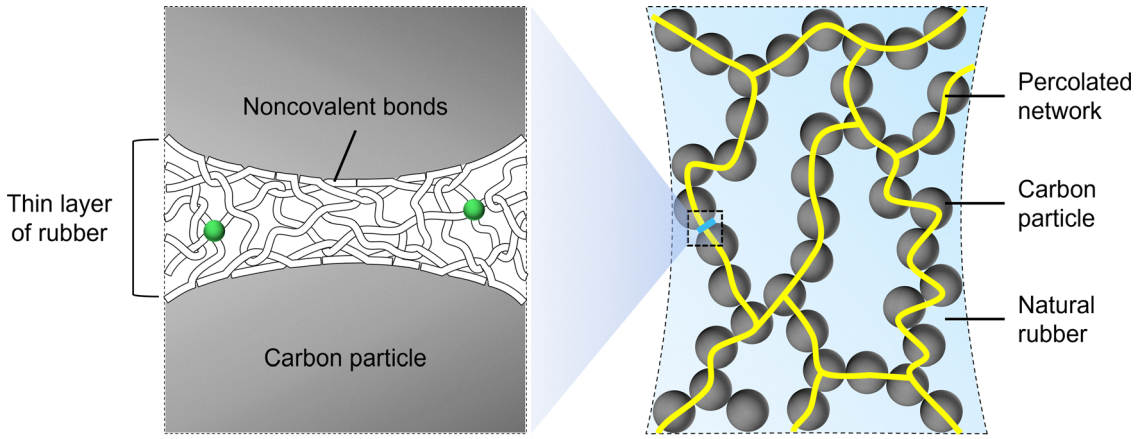

Fig. 1 Carbon black reinforced natural rubber. Carbon particles and rubber chains form strong noncovalent bonds. Above a certain volume fraction, carbon particles form a percolated network, which interpenetrates with the crosslinked network of natural rubber. Between two nearby carbon particles is a gap occupied by rubber.

not succeeded in preparing carbon black reinforced natural rubber without cutting chains.[23,24,28]

Here we hypothesize that, for carbon black reinforced natural rubber, toughness can be markedly enhanced, while maintaining modulus, by preserving long chains. We test this hypothesis by preparing a model system of carbon black reinforced natural rubber tanglemer (Fig. 1). In the model system, the size of a carbon particle is about 230 nm. Through the noncovalent bonds between carbon particles and rubber chains, each carbon particle immobilizes rubber chains within a layer of a few nanometers thick.[29,33,34] Above a certain volume fraction, carbon particles form a percolated network. Between two nearby carbon particles is a gap occupied by rubber. The thickness of the gap is larger than that of the immobilized rubber, but smaller than the size of a carbon particle. Consequently, above a certain volume fraction, carbon black reinforced natural rubber consists of two interpenetrating networks: a network of crosslinked rubber chains and a network of percolated carbon particles. These two networks form strong noncovalent bonds.

In carbon black reinforced natural rubber tanglemer, modulus is maintained by dense entanglements of natural rubber chains, as well as by the percolated network of carbon particles.

High toughness originates from energy dissipation at multiple length scales. At the tens of nanometer scale, a crack impinges on a strand of natural rubber between nearby crosslinks (Fig. 2a). Because the noncovalent bonds between strands are much weaker than the covalent bonds along the strand, the strand readily slips, deconcentrating high tension along the entire length of the strand. Consequently, rupture of a single

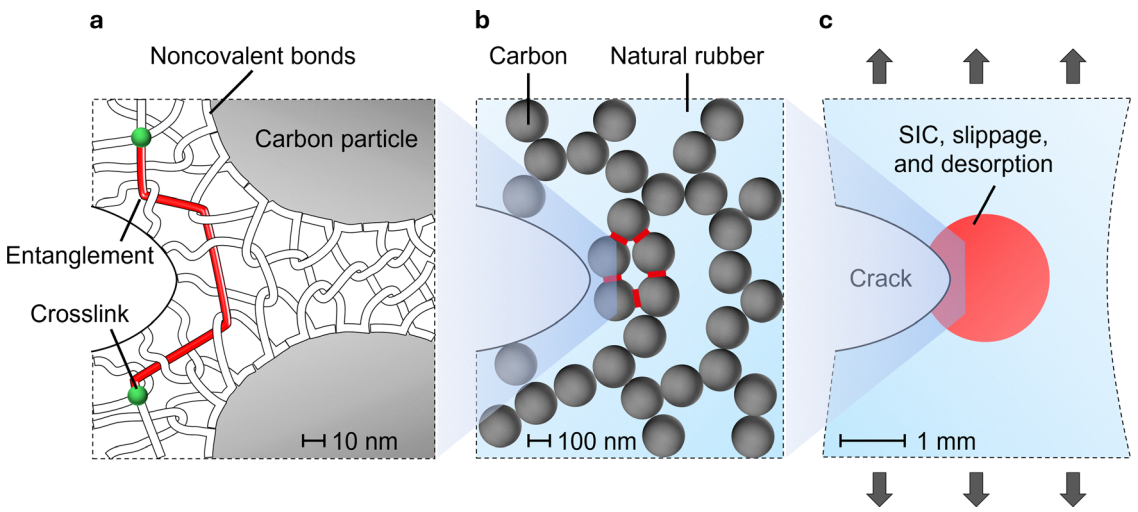

Fig. 2 In carbon black reinforced natural rubber, high toughness originates from energy dissipation at multiple length scales. (a) Near a crack tip, before a strand breaks, high tension deconcentrates along the entire length of the strand. The rubber chains and carbon particles slip and desorb. (b) High tension transmits to rubbers in nearby carbon–carbon gaps. (c) Strain-induced crystallization, as well as interfacial slip and desorption, occur in a large zone around the crack tip.

covalent bond of the strand dissipates the energy stored in every covalent bond along the strand. The sparser the crosslinks, the longer the strand, and the more energy dissipated. The rubber in the gap between two nearby carbon particles is triaxially constrained,[25,32,35] which resists tension but allows shear. High tension develops in the rubber in the gap. Under sufficiently large strain, rubber chains slip and desorb from carbon particles, dissipating energy by breaking noncovalent bonds.

At the micrometer scale, strong noncovalent bonds between carbon and rubber transmit high tension to rubbers in multiple nearby gaps through the percolated network of carbon particles. (Fig. 2b). The slip and desorption at carbon–rubber interfaces in a single gap dissipates the energy stored in many nearby gaps.

At the millimeter scale, in a zone around the crack tip, most strands do not break (Fig. 2c). As the crack advances, long strands crystallize ahead of the crack tip and melt behind the crack tip, which dissipates energy. Meanwhile, interfacial slippage and desorption between rubber chains and carbon particles also dissipate energy.

To test the hypothesis, we first compare two types of carbon black reinforced natural rubber: one with cut chains and the other with uncut chains (Fig. 3). Both have the same volume fraction of carbon particles, $F = 0.4$, and the same crosslink density, $C = 10^{-3}$. C is defined as the molar ratio between the initiator and repeat units per polyisoprene chain. For the composite with cut chains, the dangling ends of short chains do not bear load,[18] and the rubber network is not well formed at a low crosslink density of $C = 10^{-3}$. Consequently, both the modulus and toughness of the composite with cut chains are much lower than those of the composite with uncut chains.

Next, to form a good rubber network, the crosslink density of the composite with cut chains is increased to $C = 10^{-2}$, while the crosslink density of the composite with uncut chains is fixed as $C = 10^{-3}$ (Fig. 4). The two composites achieve comparable moduli but greatly different values of toughness. The results in Fig. 3 and 4 highlight that carbon black reinforced natural rubber with long chains and sparse crosslinks greatly amplifies toughness, while maintaining modulus. The remainder of the paper describes the synthesis and properties in detail.

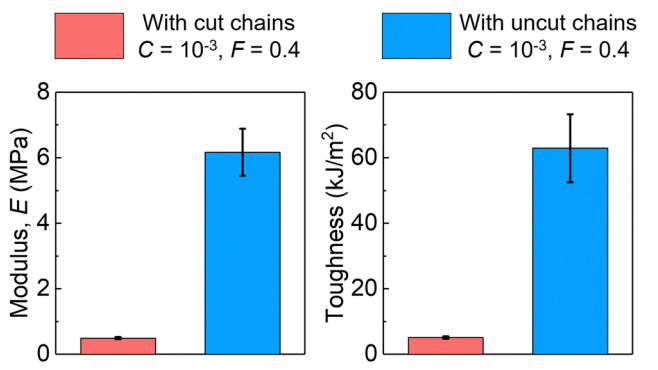

Fig. 3 Modulus and toughness of carbon black reinforced natural rubber with cut chains and with uncut chains. Both composites have the same $C = 10^{-3}$ and $F = 0.4$. All values represent averages with standard deviations for $N = 3$ replicates.

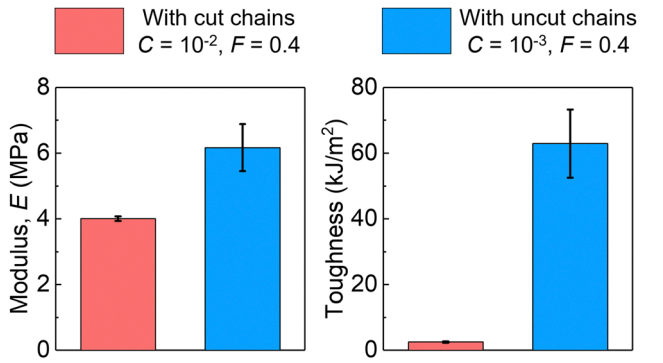

Fig. 4 Modulus and toughness of carbon black reinforced natural rubber with cut chains ($C = 10^{-2}$) and with uncut chains ($C = 10^{-3}$). Both composites have the same $F = 0.4$. All values represent averages with standard deviations for $N = 3$ replicates.

2. Conventional method to make a product of carbon black reinforced natural rubber

To set the background for this work, recall the conventional method to make a product of carbon black reinforced natural rubber (Fig. 5). Latex tapped from trees is a milky white fluid, consisting of particles of polyisoprene chains dispersed in water.[9] The chains in the latex have a high molecular weight of $\sim$1 000 000 g mol^{-1}.[1,2] The chains are hydrophobic, but are terminated with non-rubber components, including proteins and phospholipids.[9] The non-rubber components are hydrophilic, and function as surfactants that stabilize the latex particles in water.[9] As water evaporates, the particles of polyisoprene chains coagulate to form neat natural rubber.[9] The neat natural rubber is then mixed with carbon particles and additives to form a compound.[36,37] Mixing is commonly conducted using high-intensity processes, such as roll milling and internal mixing, subjecting the compound to severe shear and elevated temperatures.[36,37] The high-intensity processes masticate rubber chains, lower viscosity, and disperse carbon particles in the rubber matrix. Mastication reduces the length of rubber chains by an order of magnitude.[10,11,38] The compound is then shaped into the geometry of a product by extrusion or molding within a window of time and temperature.[36,37] Subsequently, the rubber chains are crosslinked into a network, in which crosslinks divide each rubber chain into multiple strands and two dangling ends. For the same crosslink density, a network of short chains has more dangling ends than a network of long chains, and the dangling ends do not bear load.[18] To compensate for this shortcoming, the short chains are densely crosslinked.[18]

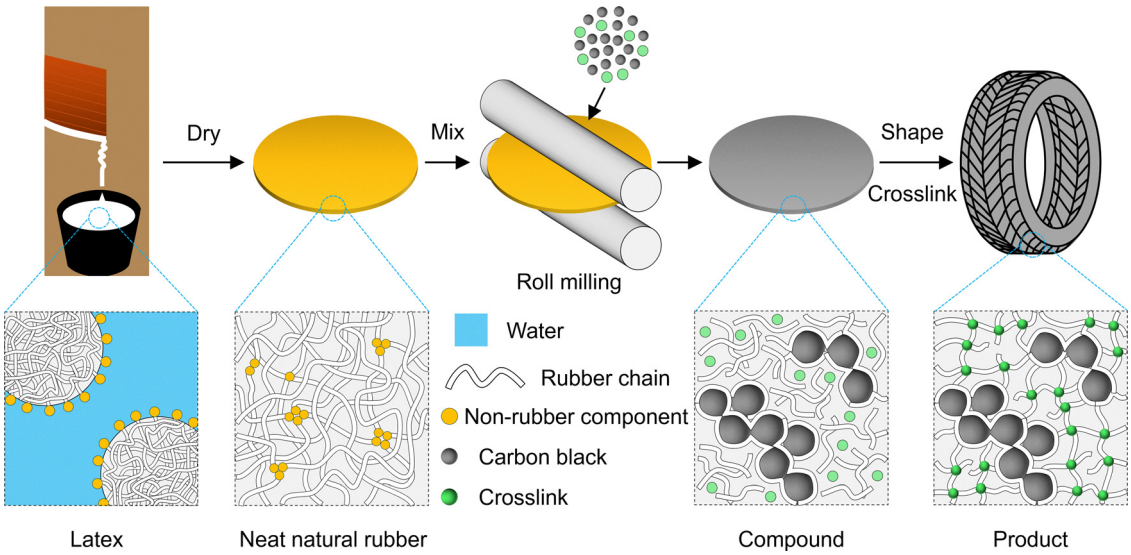

Fig. 5 A conventional method to make a product of carbon black reinforced natural rubber involves several steps, which change the molecular architecture of rubber chains.

3. Solution process to make carbon black reinforced natural rubber tanglemer

To preserve long chains, we begin with latex (Fig. 6a). We dissolve the thermal initiator, dicumyl peroxide (DP), in toluene (Fig. 6b). The DP-toluene solution is mixed with latex to dissolve the latex particles into polyisoprene chains (Fig. 6c). Water remains in a trace amount (5 vol%) and likely surrounds the non-rubber components.

Separately, we disperse carbon black particles in toluene (Fig. 6d). The carbon particles used in this work are not fused as aggregates and can be uniformly dispersed in toluene. The carbon–toluene dispersion is then mixed with the DP-toluene-water–rubber solution to uniformly disperse carbon particles without cutting the rubber chains (Fig. 6e). The homogenized mixture is left at room temperature to fully evaporate toluene and water (Fig. 6f). As evaporation proceeds, strong noncovalent bonds form between carbon particles and rubber chains, and rubber chains in the matrix entangle.

The dried mixture, called a compound, is shaped at 90 °C for 1 hour. The temperature and time are chosen such that during shaping the rubber chains are uncut and uncrosslinked. The compound is then cured at 140 °C for 3 hours. During curing, DP decomposes into free radicals. Each DP molecule creates a crosslink between rubber chains[36] (Fig. 6g). Thus, we take the molar ratio between DP and repeat units per polyisoprene chain, C, as the crosslink density.

After curing, carbon particles are uniformly distributed in the rubber matrix, confirmed by scanning electron microscope (SEM) images of the cross sections of the sample (Fig. 7). The carbon particles used in this work are not fused as aggregates.

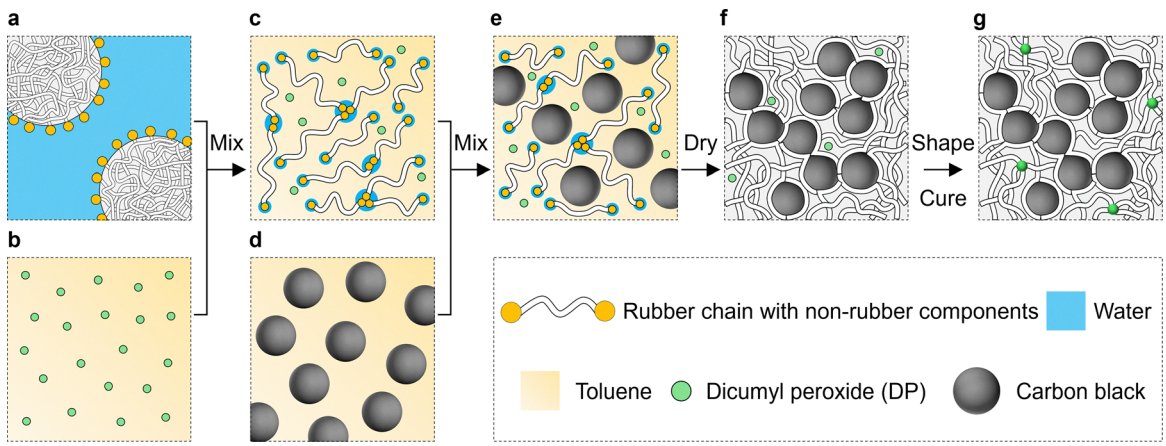

Fig. 6 Solution process to make carbon black reinforced natural rubber with long chains. (a) Latex. (b) DP-toluene solution. (c) Mixture of polyisoprene chains, water, toluene, and DP. (d) Suspension of carbon particles in toluene. (e) Mixture of polyisoprene chains, water, toluene, DP, and carbon particles. (f) Uncured compound. (g) Cured carbon black reinforced natural rubber.

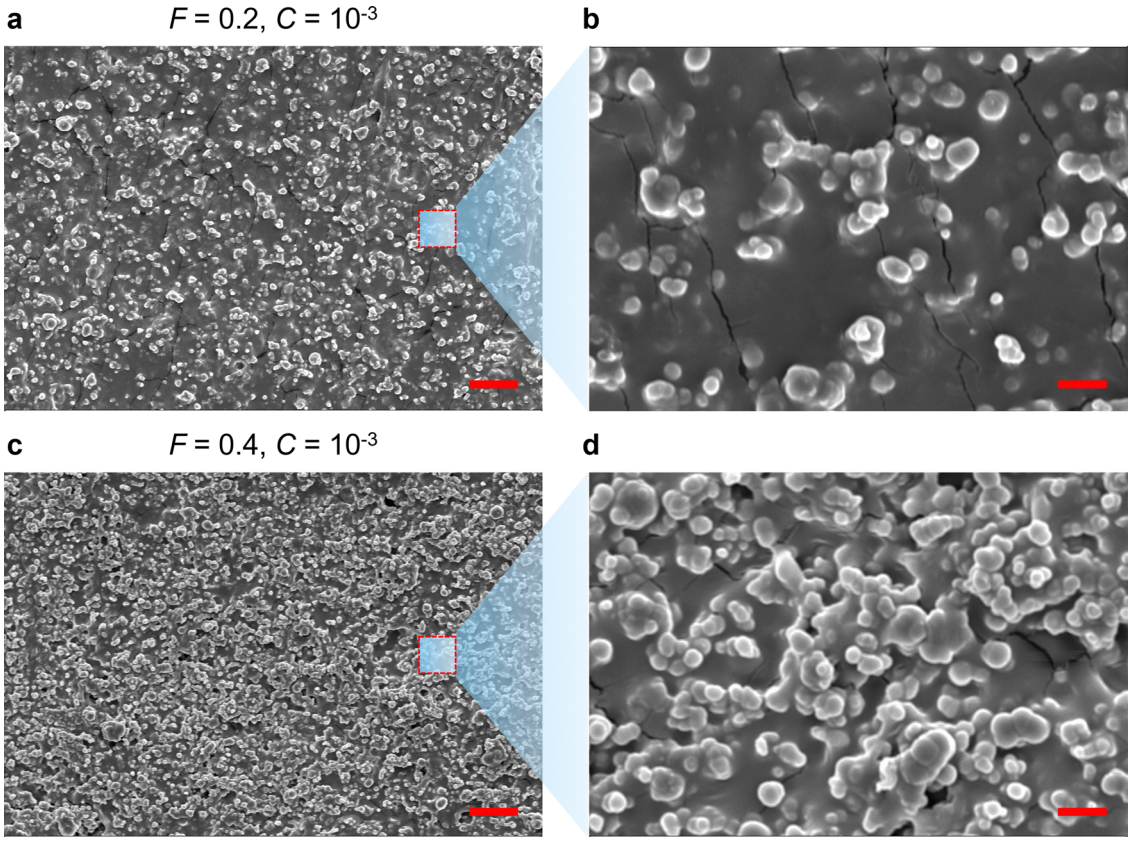

Fig. 7 Distribution of carbon particles in natural rubber. Scanning electron microscope (SEM) images of the cross section of the composite with $F = 0.2$ and $C = 10^{-3}$: (a) Scale bar, 5 μm, and (b) Scale bar, 1 μm. SEM images of the cross section of the composite with $F = 0.4$ and $C = 10^{-3}$: (c) Scale bar, 5 μm, and (d) Scale bar, 1 μm.

The diameter of a particle is about 230 nm. Because the rubber chains and carbon particles form strong noncovalent bonds, carbon particles absorb rubber chains. The particles distribute uniformly at a length scale larger than an individual particle, but form clusters in which particles are closer to one another than average. In a cluster, two nearby particles do not touch each other directly, but are separated by a thin gap occupied by rubber. As the volume fraction of carbon particles increases, they form larger and larger clusters until they percolate. After percolation, the composite forms two interpenetrating networks: the network of crosslinked rubber chains, and the network of percolated carbon particles (Fig. 1, right). The two networks adhere to each other through noncovalent bonds. The particles do not percolate at a low volume fraction of particles $F = 0.2$ (Fig. 7a and b), but percolate at a high volume fraction $F = 0.4$ (Fig. 7c and d). These observations are consistent with the well-established percolation threshold of rigid particles, which typically occurs at a volume fraction of approximately $F = 0.24$ to 0.3.[39–41]

To prepare a composite with cut chains, the compound is passed 100 times through a two-roll mill with a 1 mm roll gap. After milling, the compound becomes sticky, indicating an increase in dangling ends. The compound is then hot-pressed at 140 °C for 3 hours. After curing, carbon particles are uniformly distributed within the rubber matrix, as confirmed by SEM images. No significant difference in the dispersion of carbon black is observed between the composites prepared by two processes: two-roll milling followed by hot pressing, and direct hot-pressing. The dangling ends in the masticated sample do not bear load, requiring a high crosslink density of $C = 10^{-2}$ to form a composite of a modulus comparable to that of the composite with uncut chains ($C = 10^{-3}$).

A tanglemer is designed with the condition:

$$n \gg n_c \gg n_e \quad (1)$$

where n is the number of repeat units per chain, n_c is the number of repeat units between two neighboring crosslinks, and n_e is the number of repeat units between two neighboring entanglements. When $n \gg n_c$, the network has far more load-bearing strands than dangling ends;[17,42] otherwise, the network is not well formed.[18] When $n_c \gg n_e$, entanglements greatly outnumber crosslinks.[17,42] For uncut natural rubber chains, $n \sim 14\,000$.[1,2] In a fully relaxed melt of uncrosslinked natural rubber chains, $n_e = 56$.[43] As we will show, the networks of long strands prepared in this work preserve this value of n_e. Importantly, because $n \gg n_e$, natural rubber offers a wide window to choose n_c that satisfies condition (1).

We estimate n_c by $1/(2C)$. When $C = 10^{-3}$, $n_c = 500$, which is more than an order of magnitude smaller than n, and about one order of magnitude larger than n_e. Therefore, a network

with crosslink density $C = 10^{-3}$ satisfies condition (1) and is a tanglemer. By contrast, when $C = 10^{-2}$, $n_c = 50$, which is comparable to n_e. Therefore, a network with crosslink density $C = 10^{-2}$ does not satisfy condition (1) and is not a tanglemer. As another example, when $C = 10^{-4}$, $n_c = 5000$, which is about one-third of n. Therefore, a network with crosslink density $C = 10^{-4}$ has a large fraction of dangling ends relative to load-bearing strands and is not well formed.

In particular, the fraction of dangling ends and load-bearing strands can be estimated from the chain length and crosslink density. Let N_c be the average number of crosslinks per chain. N_c divides the chain into $(N_c + 1)$ strands, with 2 dangling strands and $(N_c - 1)$ load-bearing strands. The fraction of load-bearing strands is therefore $\varphi = (N_c - 1)/(N_c + 1)$. N_c is calculated as $N_c = n/n_c$. For uncut natural rubber chains, $n \sim 14\,000$. At $C = 10^{-3}$, we obtain $n_c = 500$, $N_c = 28$, and $\varphi = 0.93$.

In this work, we prepare networks with C ranging from $C = 10^{-3}$ to $C = 10^{-2}$, so that all networks satisfy $n \gg n_c$ and have small fractions of dangling ends. Networks with high crosslink densities ($C = 5 \times 10^{-3}$ and 10^{-2}) do not satisfy $n_c \gg n_e$ but are included for comparison.

4. Rheology

We measure the storage modulus E' and loss modulus E'' using a dynamic mechanical analyzer. The strain sweeps from 0.1% to 10% at a constant frequency of 1 Hz and a temperature of 25 °C. Three materials are tested: neat natural rubber ($F = 0$), composite with unpercolated carbon particles ($F = 0.2$), and composite with percolated carbon particles ($F = 0.4$). All samples have the same low crosslink density of $C = 10^{-3}$.

For neat natural rubber, both E' (Fig. 8a) and E'' (Fig. 8b) are nearly constant, independent of the amplitude of strain. Similar behavior is observed for the composite with unpercolated particles ($F = 0.2$). For the composite with percolated particles ($F = 0.4$), both E' and E'' are much higher at a small strain of ~0.1%, but decrease with increasing strain.

The ratio of the loss modulus to the storage modulus, E''/E', measures dissipation of a material (Fig. 8c). For neat natural rubber and the composite with unpercolated particles, the dissipation is low, $E''/E' \sim 0.1$, and is nearly constant, independent of the amplitude of strain. For the composite with percolated carbon particles, the dissipation is higher, $E''/E' \sim 0.2$ to ~ 0.3.

The behavior of neat natural rubber is well known.[3,17,44] Natural rubber is highly stretchable and remains linear elastic under strain up to ~10% in the DMA test. Thus, the storage modulus E' is constant, independent of the amplitude of strain. The constant storage modulus E' is consistent with entropic elasticity, estimated by[17,44]

$$E' = \frac{3\rho RT}{2M_0}\left(\frac{1}{n_e} + \frac{1}{n_c}\right) \quad (2)$$

where ρ is the density of the polymer, R is the universal gas constant, T is the temperature, and M_0 is the molecular weight of a repeat unit.

At $C = 10^{-3}$, the network satisfies $n \gg n_c \gg n_e$, and is a tanglemer. Consequently, entanglements set the modulus, $E' \sim 1/n_e$.[17,42] This conclusion is further supported by the finding that the storage modulus of the crosslinked network of neat natural rubber, $E' \sim 0.93$ MPa, is approximately the plateau modulus of the melt of uncrosslinked natural rubber chains.[7] For the neat natural rubber, the ratio E''/E' is constant and low because the noncovalent bonds between natural rubber chains are weak, and because the amplitude of strain is too small to activate SIC.

The noncovalent carbon–rubber bonds are strong, so that individual carbon particles are covered by rubber chains (Fig. 1a, left). A carbon particle immobilizes rubber chains within a layer of a few nanometers,[29,33,34] much smaller than the ~230 nm diameter of a carbon particle. Within a cluster or the percolated network of carbon particles, between two nearby carbon particles is a gap occupied by rubber. The thickness of the gap is small compared to the diameter of an individual particle but is large compared to the thickness of the layer of immobilized rubber. The rubber in the gap is triaxially constrained,[35] which resists separation in the direction normal to the gap, but allows shear in the direction tangent to the gap. Because the volume fraction of immobilized rubber chains is small, their immobility has a small effect on the modulus of the

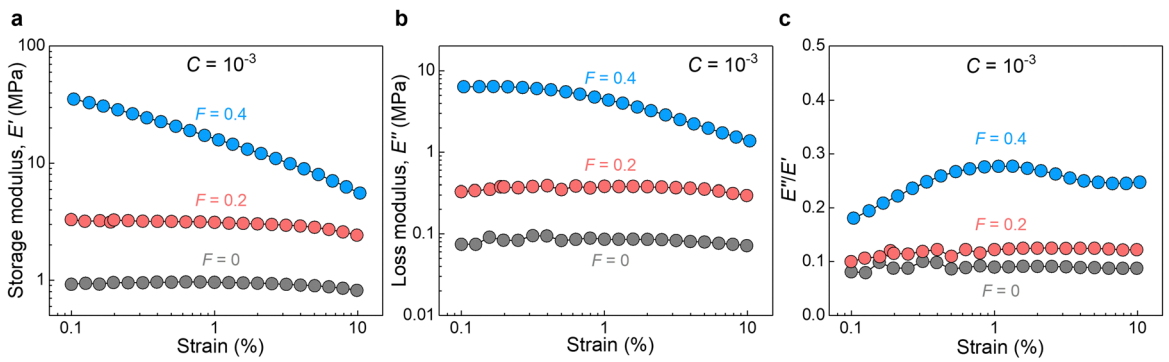

Fig. 8 Rheology of neat natural rubber and carbon black reinforced natural rubber. (a) Storage modulus, E'. (b) Loss modulus, E''. (c) The ratio of the loss modulus to the storage modulus, E''/E'. Three materials are tested: neat natural rubber ($F = 0$), composite with unpercolated carbon particles ($F = 0.2$), and composite with percolated carbon particles ($F = 0.4$). All samples have the same crosslink density of $C = 10^{-3}$.

composite. By contrast, the triaxially constrained gaps of rubber chains greatly amplify the modulus of the composite.

At F = 0.2, carbon particles cluster but do not percolate (Fig. 7a and b). The gaps between clusters are large compared to the gaps between nearby particles within a cluster, so that the rubber in the former is less triaxially constrained than the rubber in the latter. The rubber within each cluster is much less deformable than the rubber between clusters. Consequently, clustering increases the effective volume fraction of rigid particles. This effect accounts for the mild increase of storage modulus relative to the neat natural rubber. Because deformation mainly takes place in the rubber between clusters, and because the strain is small enough that carbon–rubber bonds remain intact, the storage modulus E' and the ratio E''/E' remain constant, independent of the amplitude of strain.

At F = 0.4, carbon particles percolate (Fig. 7c and d). Two nearby carbon particles resist separation in the direction normal to the gap but allow shear in the direction tangent to the gap. Consequently, the percolated network of carbon particles is much stiffer than neat rubber. The two interpenetrating networks account for the ~30 times increase of storage modulus relative to the neat natural rubber at a small strain of 0.1%. With the increase of strain, high tension develops in the rubber in the gap between nearby carbon particles. When two nearby carbon particles are pulled to separate, the rubber in the gap slides relative to carbon particles. The rubber may even detach or form cavities.[25,32,35,45] The breaking of the network of percolated carbon particles reduces both storage and loss moduli, and also increases the energy dissipation with a larger E''/E'.

5. Stress–stretch curves

We measure the stress–stretch curves of the composites with unpercolated carbon particles, F = 0.2, at various crosslink densities: $C = 10^{-3}$, 2×10^{-3}, 3×10^{-3}, 5×10^{-3}, 10^{-2} (Fig. 9a). When $C \leq 3 \times 10^{-3}$, the stretchability decreases mildly with increasing C. When $C > 3 \times 10^{-3}$, the stretchability decreases significantly with increasing C. We calculate the modulus by linearly fitting the slope of the stress–stretch curve at small stretch ($\lambda < 1.03$). When $C \leq 3 \times 10^{-3}$, the modulus plateaus (Fig. 9b). With further increase of C, the modulus increases significantly. This trend is similar to that of the neat natural rubber (Fig. 9b, red).[7]

The change of modulus with C is interpreted as follows. First, when $C \leq 3 \times 10^{-3}$, the condition $n \gg n_c \gg n_e$ is satisfied, and the network of natural rubber is a tanglemer. Thus, the modulus plateaus, set by entanglements. Considering that $n_c = 1/(2C)$ and $n_e = 56$, the number of trapped entanglements between two crosslinks is $N_e = n_c/n_e$. In the plateau region, N_e increases from ~3 to ~9 as C decreases from 3×10^{-3} to 10^{-3}. These trapped entanglements act as the main load-bearing junctions in this regime, giving rise to the observed modulus plateau. Second, when $C > 3 \times 10^{-3}$, the condition $n_c \gg n_e$ is not satisfied. In this regime, the crosslink density is comparable to the entanglement density, and the network of natural rubber is not a tanglemer. Thus, the modulus rises, set by crosslinks. Third, as discussed in the section on rheology, at F = 0.2, carbon particles form clusters, but do not percolate. Clustering increases the effective volume fraction of carbon particles. Consequently, the modulus of the composite scales with that of neat rubber and is higher by a factor of 2–3. Whenever the modulus of neat rubber is increased, so is the modulus of the composite. This scaling results from continuum theory of composites.[46]

The area under the stress–stretch curve up to rupture defines the work of fracture, W_c. When $C \leq 3 \times 10^{-3}$, W_c plateaus. When $C > 3 \times 10^{-3}$, W_c decreases significantly with increasing C (Fig. 9c).

Next, we measure the stress–stretch curves of the composites with percolated carbon particles, F = 0.4, at various crosslink densities (Fig. 10a). When $C \leq 3 \times 10^{-3}$, the stretchability decreases mildly with increasing C. When $C > 3 \times 10^{-3}$, the stretchability decreases significantly with increasing C. When $C \leq 3 \times 10^{-3}$, the modulus plateaus (Fig. 10b). With further increase of C, the modulus increases significantly. This trend is similar to that of the neat natural rubber (Fig. 10b, red).[7]

The change of modulus with C is interpreted as follows. When $C \leq 3 \times 10^{-3}$, the modulus plateaus, set by entanglements. When $C > 3 \times 10^{-3}$, the modulus rises, set by crosslinks. Furthermore, as discussed in the section on rheology, at

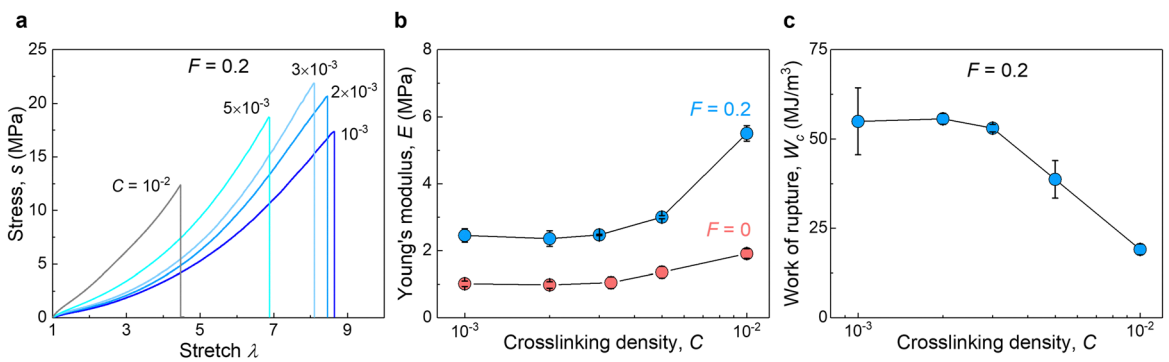

Fig. 9 Uniaxial tensile tests of composites with unpercolated carbon particles (F = 0.2) at various crosslink densities C. (a) Stress–stretch curves. (b) Young's modulus E. Data for neat natural rubber (F = 0) is extracted from our previous study.[7] (c) Work of rupture, W_c. Values in (b) and (c) represent averages with standard deviations for N = 3 replicates.

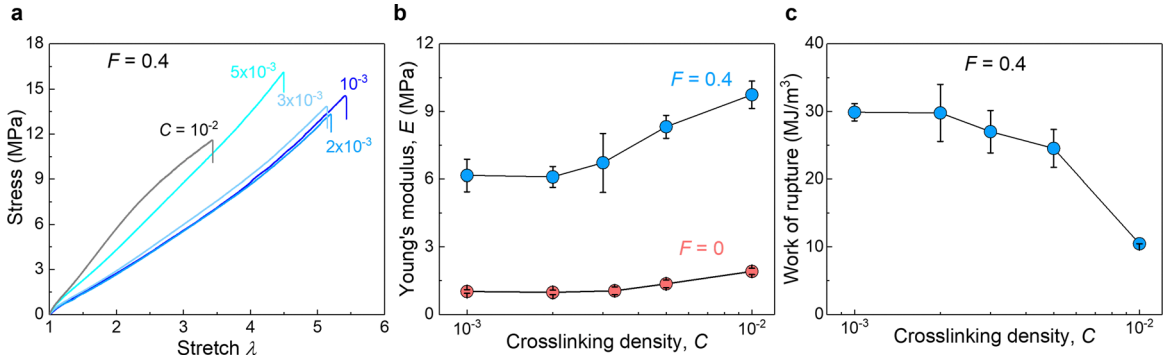

Fig. 10 Uniaxial tensile tests of composites with percolated carbon particles (F = 0.4) at various crosslink densities C. (a) Stress–stretch curves. (b) Young's modulus E. Data for neat natural rubber (F = 0) is extracted from our previous study.[7] (c) Work of rupture, W_c. Values in (b) and (c) represent averages with standard deviations for N = 3 replicates.

$F = 0.4$, carbon particles form a percolated network that is much stiffer than neat rubber. The modulus of the percolated network still scales with that of neat rubber. Whenever the modulus of neat rubber is increased, so is the modulus of the composite. However, the scaling behavior differs between composites with unpercolated and percolated particles.[47,48] Consequently, at $F = 0.4$, the modulus of the composite is 5 to 7 times that of neat natural rubber.

Furthermore, when $C \leq 3 \times 10^{-3}$, W_c plateaus. When $C > 3 \times 10^{-3}$, W_c decreases with the increase of C (Fig. 10c).

6. Strain-induced crystallization

We use wide-angle X-ray scattering (WAXS) to study SIC of carbon black reinforced natural rubber under uniaxial stretch. One-dimensional (1D) WAXS intensity profiles are deconvoluted into amorphous and crystalline peaks using a Gaussian function. In the analysis, the contribution from carbon black is decoupled. That is, crystallinity is defined by the volume fraction of rubber that crystallizes, $\chi_c = A_c/(A_c + A_A)$, where A_c and A_A are the total integrated area of fitted crystalline and amorphous peaks of natural rubber, respectively.

We first study composites with unpercolated carbon particles (F = 0.2) at two different crosslink densities: $C = 10^{-3}$ and $C = 10^{-2}$ (Fig. 11). For both composites, in the undeformed state ($\lambda = 1$), 1D WAXS intensity profiles show two broad peaks corresponding to amorphous rubber, and carbon black (Fig. 11a and b). As stretch exceeds 2, distinct peaks emerge, indicating the onset of crystalline formation. These peak intensities increase with increasing stretch, indicating progressive crystalline formation. At $\lambda = 6.6$, close to rupture, the composite with a low crosslink density ($C = 10^{-3}$) reaches a maximum crystallinity of $\chi_c \sim 28\%$ (Fig. 11c). However, at $\lambda = 4$, close to rupture, the composite with a high crosslink density ($C = 10^{-2}$) only reaches a maximum crystallinity of $\chi_c \sim 15\%$. As a comparison, we also include the data for neat natural rubber extracted from our previous study.[7]

The experimental findings are interpreted as follows. First, SIC occurs when rubber strands are stretched to alignment. At each point of entanglement or crosslink, SIC cannot occur. Entanglements within the rubber network can redistribute stress by sliding along strands, unlike crosslinks which restrict movement of strands. The composite with a low crosslink density has a larger stretchability than the composite with a high crosslink density, enabling a higher maximum

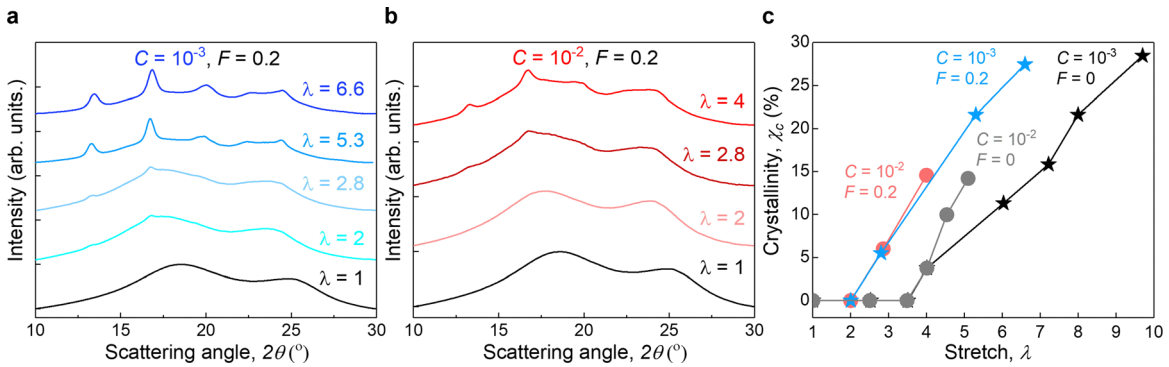

Fig. 11 Strain-induced crystallization of composites with unpercolated carbon particles, F = 0.2. One dimensional WAXS intensity profiles showing crystalline peaks at different stretches for (a) $C = 10^{-3}$. (b) $C = 10^{-2}$. (c) Crystallinity (χ_c) as a function of stretch (λ). Data for neat natural rubber (F = 0) is extracted from our previous study.[7]

crystallinity. This effect is consistent with the trend that lower crosslink density enhances crystallinity.[7,49,50]

Second, compared to neat natural rubber,[6,7] the addition of carbon particles lowers the onset stretch of SIC.[32] The network of crosslinked rubber chains adheres to the cluster of carbon particles through strong noncovalent bonds.[23,24,28,29] These noncovalent bonds constrain rubber chains near the surface of carbon particles. These constrained chains require less deformation to reach the critical alignment for crystallization, promoting earlier onset of SIC.[30–32,51] Meanwhile, stress concentration around carbon particles also amplifies local strain in the surrounding rubber matrix, facilitating earlier nucleation of crystalline domains.[30–32,51] As a result, SIC begins at a lower stretch in the composite than in neat natural rubber.

Third, within each cluster, rubber chains in the thin gap between two nearby carbon particles are triaxially constrained,[35] cannot freely align, and are less able to crystallize. At $F = 0.2$, the volume fraction of such constrained rubber is low. Consequently, the maximum crystallinity of the composite ($\chi_c \sim 28\%$) remains comparable to neat natural rubber ($\chi_c \sim 30\%$).[7]

Next, we study composites with percolated carbon particles ($F = 0.4$) at two crosslink densities: $C = 10^{-3}$ and $C = 10^{-2}$ (Fig. 12). For both composites, in the undeformed state ($\lambda = 1$), 1D WAXS intensity profiles show two broad peaks (Fig. 12a and b). As stretch exceeds 2, distinct peaks emerge. These peak intensities increase with increasing stretch. At $\lambda = 4.9$ close to rupture, the composite with a low crosslink density reaches a maximum crystallinity of $\chi_c \sim 20.9\%$ (Fig. 12c). However, at $\lambda = 2.9$ close to rupture, the composite with a high crosslink density only reaches a maximum crystallinity of $\chi_c \sim 7.1\%$. As a comparison, we also include the data for neat natural rubber extracted from our previous study.[7]

The experimental findings are interpreted as follows. First, the composite with a low crosslink density has a larger stretchability than the composite with a high crosslink density, enabling a higher maximum crystallinity. Second, compared to neat natural rubber, carbon particles lower the onset stretch of SIC. Third, rubber chains in the thin gap between two nearby carbon particles are triaxially constrained, which cannot freely align and are less able to crystallize. At $F = 0.4$, the volume fraction of such constrained rubber is increased. Consequently, the maximum crystallinity of the composite ($\chi_c \sim 20.9\%$) is lower than that of neat natural rubber ($\chi_c \sim 30\%$).[7]

Notably, compared to our prior work on silica reinforced natural rubber tanglemer,[22] carbon black reinforced natural rubber has a higher maximum crystallinity. In silica reinforced natural rubber, silica particles are covalently interlinked with rubber chains, which restrict chain mobility, hinder alignment, and suppress SIC.[30,31,52–54] By contrast, carbon black interacts with rubber chains through noncovalent bonds.[23,24,28,29] These noncovalent bonds are weaker than covalent bonds along rubber chains. Under sufficient stress, rubber chains can slip and desorb from the surface of carbon particles. Once detached, these chains extend and align, promoting further development of SIC.

7. Mullins effects

We study Mullins effects of composites with unpercolated carbon particles ($F = 0.2$) at two different crosslink densities: $C = 10^{-3}$ and $C = 10^{-2}$. Each composite is loaded to increasing stretches and then unloaded in sequence (Fig. 13a and b). Hysteresis is defined as the ratio of the area enclosed by the loading–unloading loop to the area under the loading curve.

For both composites, hysteresis increases with stretch (Fig. 13c). The composite with a low crosslink density ($C = 10^{-3}$) shows larger hysteresis than the composite with a high crosslink density ($C = 10^{-2}$).

The increased hysteresis at stretches above $\lambda = 2$ arises from several mechanisms.[23,24,28,29] First, when stretch exceeds $\lambda = 2$, SIC occurs. The formation and melting of SIC dissipates energy. Second, as stretch increases, rubber chains slip and desorb from carbon surfaces, further increasing hysteresis. Third, higher stretch promotes chain scission, leading to larger hysteresis.

The composite with a low crosslink density has longer strands than the composite with a high crosslink density. Long strands exhibit greater chain friction, more irreversible network rearrangement, and slower elastic recovery. As a result, hysteresis increases. By contrast, the composite with a high crosslink

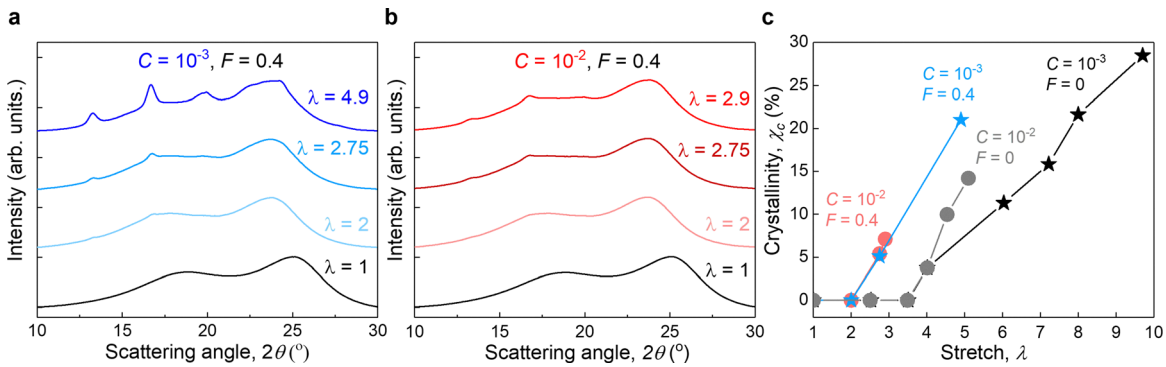

Fig. 12 Strain-induced crystallization of composites with percolated carbon particles, $F = 0.4$. One dimensional WAXS intensity profiles showing crystalline peaks at different stretches for (a) $C = 10^{-3}$. (b) $C = 10^{-2}$. (c) Crystallinity (χ_c) as a function of stretch (λ). Data for neat natural rubber ($F = 0$) is extracted from our previous study.[7]

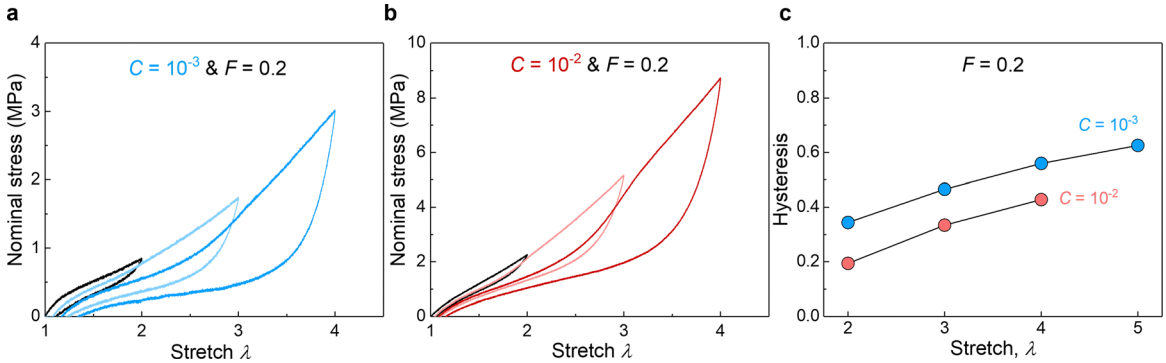

Fig. 13 Mullins effects of composites with unpercolated carbon particles (F = 0.2). (a) C = 10^{-3}. (b) C = 10^{-2}. (c) Hysteresis as a function of stretch.

density behaves more elastically and recovers efficiently, reducing hysteresis.

We next study Mullins effects of composites with percolated carbon particles (F = 0.4) at two different crosslink densities: C = 10^{-3} and C = 10^{-2} (Fig. 14a and b). For the composite with a low crosslink density, hysteresis remains high. For the composite with a high crosslink density, hysteresis increases with stretch (Fig. 14c). Again, the composite with a low crosslink density shows larger hysteresis than the composite with a high crosslink density.

As mentioned above, hysteresis arises from chain friction, formation and melting of SIC, interfacial slippage and desorption of rubber chains from carbon particles, and chain scission.[23,24,28,29]

Notably, at small stretch, *e.g.*, λ = 2, the composites with percolated carbon particles (F = 0.4) exhibit much larger hysteresis than the composites with unpercolated carbon particles (F = 0.2). At F = 0.2, carbon particles form clusters, but do not percolate. At small stretches, deformation is mainly accommodated by the rubber between clusters, while carbon–rubber bonds largely remain intact and SIC has not been extensively activated, resulting in low hysteresis (Fig. 13c). In contrast, at F = 0.4, carbon particles form a percolated network. Even at small stretches, high tension develops in the triaxially constrained rubber between nearby carbon particles, causing carbon–rubber bonds to break even though SIC has not yet been extensively activated. Consequently, the percolated carbon network breaks more extensively under the same stretch, leading to much larger hysteresis (Fig. 14c).

8. Toughness

We measure the toughness of carbon black reinforced natural rubber using the pure shear test. We compare two composites with percolated carbon particles (F = 0.4). At a high crosslink density (C = 10^{-2}), the notched sample fractures catastrophically at λ_c = 1.26 (Fig. 15a). At a low crosslink density (C = 10^{-3}), the notched sample bifurcates the crack at λ = 1.82, and resists the further crack propagation until reaching the critical stretch of λ_c = 3.51 (Fig. 15b).

For composites with unpercolated carbon particles (F = 0.2), toughness increases by ~40 times, from ~2.5 kJ m^{-2} at C = 10^{-2} to ~100 kJ m^{-2} at C = 10^{-3} (Fig. 15c). For composites with percolated carbon particles (F = 0.4), toughness increases by more than an order of magnitude, from ~3.5 kJ m^{-2} at C = 10^{-2} to ~63 kJ m^{-2} at C = 10^{-3}. The fractocohesive length, defined as the ratio of the toughness to the work of fracture,[55,56] also decreases with the increase of the crosslink density for both composites (Fig. 15d). Compared to many commonly used unfilled rubbers and carbon black reinforced rubbers, the carbon black reinforced natural rubber tanglemers developed in this study exhibit higher toughness while retaining comparable modulus (Fig. 15e).

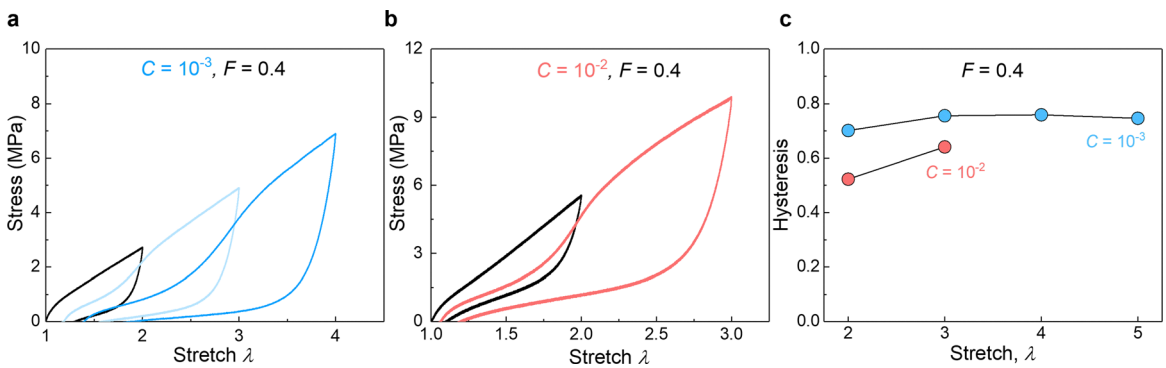

Fig. 14 Mullins effects of composites with percolated carbon particles (F = 0.4). (a) C = 10^{-3}. (b) C = 10^{-2}. (c) Hysteresis as a function of stretch.

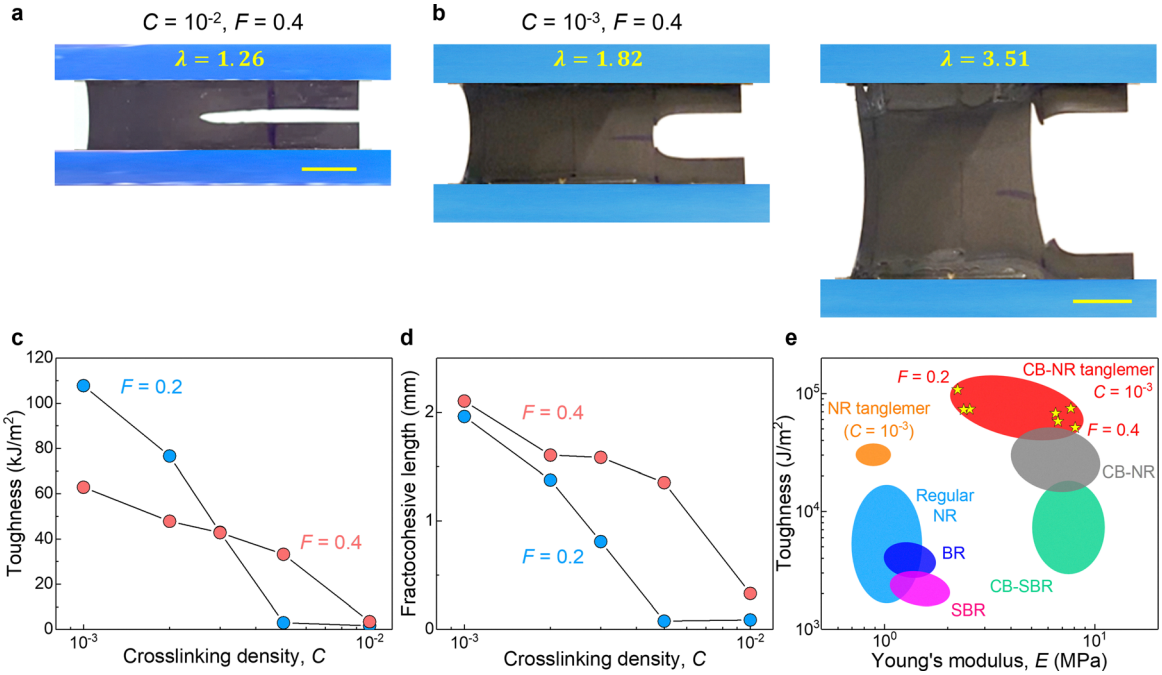

Fig. 15 Toughness. Crack propagation for the composites with (a) $C = 10^{-2}$ and $F = 0.4$, and (b) $C = 10^{-3}$ and $F = 0.4$. (c) Toughness, and (d) fractocohesive length as a function of C. (e) Carbon black reinforced natural rubber tanglemer compared with rubbers on the plane of toughness and Young's modulus E. NR: natural rubber; BR: butadiene rubber; SBR: styrene-butadiene rubber; CB-SBR: carbon black reinforced SBR; and CB-NR: carbon black reinforced natural rubber. NR tanglemer is prepared using the similar solution process in Fig. 6. Scale bars: 1 cm.

These results support the proposed mechanism of multiscale dissipation (Fig. 2). High toughness originates from energy dissipation across multiple length scales: along long rubber strands, across clustered carbon particles, and within a zone of SIC as well as slip and desorption at carbon–rubber interfaces. Near the crack tip, before a long strand breaks, high tension is transmitted along its entire length. Before the rubber in a thin gap between two carbon particles ruptures, high tension is transmitted to rubber in many nearby gaps between carbon particles in a cluster. Consequently, SIC and slip and desorption occur within a large zone around the crack tip. The processes at the three length scales are synergetic. The deconcentration of high tension over long rubber strands and over multiple gaps in clustered particles enlarges the zone of SIC and interfacial slip and desorption. The large zone of dissipation, in turn, shields the strands and clusters near the crack tip from the applied load. This synergy of dissipative processes near the crack tip and background is analogous to the synergy in other classes of materials, including metals[57] and ceramic matrix composites.[58]

Our experimental results are consistent with the proposed mechanism of multiscale dissipation (Fig. 2). First, the composite with a lower crosslink density has longer strands. The toughness of the composite increases as the crosslink density decreases (Fig. 15c). This finding is consistent with the expectation that longer strands dissipate more energy upon rupture. Second, the composite with a lower crosslink density achieves higher maximum crystallinity (Fig. 11c and 12c). This finding is consistent with the previous reports that long strands, on stretching, ease alignment and crystallization.[7,49,50] The more extensive the crystallization and melting, the more energy dissipated, amplifying toughness. Third, the fractocohesive length scales the size of the fracture process zone where SIC and interfacial slip and desorption occur. The composite with a lower crosslink density has a larger fractocohesive length (Fig. 15d). This is consistent with the notion of synergy between the strands and clusters at the crack tip and the zone of dissipation in the background.

Notably, at the same low crosslink density ($C = 10^{-3}$), the composite with unpercolated carbon particles, $F = 0.2$, shows higher toughness ($\sim$100 kJ m^{-2}) than the composite with percolated carbon particles, $F = 0.4$, ($\sim$63 kJ m^{-2}). We attribute this difference to the higher maximum crystallinity in the former, as discussed in the section on SIC.

9. Concluding remarks

Nature synthesizes long rubber chains of high molecular weight.[1,2] These long chains are often considered a drawback for processing because their high viscosities make mixing difficult. To overcome this challenge, high-intensity processes such as roll milling or internal mixing are widely used to mix carbon black, additives, and rubber chains.[36,37] These processes cut rubber chains.[10,11,38] The shortened chains improve processability but degrade the performance of the composites.[18]

Here we show that, when long chains of natural rubber are preserved and sparsely crosslinked, the composite amplifies

toughness while maintaining modulus. The combination of modulus and toughness in our material arises from the interpenetration of two networks: the crosslinked rubber chains and the percolated carbon particles. The two networks adhere through strong noncovalent bonds. Dense entanglements set the modulus of the sparsely crosslinked rubber matrix. The percolated network of carbon particles triaxially constrains rubber chains in the interparticle gaps, amplifying modulus. Preserving long chains markedly amplifies toughness due to the multiscale energy dissipation across long strands, carbon particles, and a zone of SIC and interfacial dissipation.

We test our hypothesis using unstructured carbon black as a model filler and peroxide as a model crosslinker. In industry, structured carbon black is widely used, which gives composites of high reinforcement at a lower volume fraction of carbon black.[23,24,28,29] We will report elsewhere on composites of structured particles and natural rubber tanglemers. Furthermore, sulfur is widely used as a crosslinker, which leads to composites of higher toughness than those crosslinked by peroxide.[6,59–62] Our previous study demonstrated that preserving long chains significantly enhances the fatigue resistance of neat natural rubber.[7] The combined effects of preserved long chains and carbon–rubber interactions on fatigue properties will be investigated in a separate study. These considerations provide ample opportunities for future study.

Manufacturing a product of synthetic rubber involves several steps: synthesizing the rubber, compounding the rubber with additives and fillers, shaping the product, and curing.[36,37] Polymers are often synthesized in solvents, whereas compounding, shaping, and curing have traditionally been performed in a solvent-free environment. This division in manufacturing products of synthetic rubbers is now being reconsidered, with solvent-assisted compounding increasingly explored and gradually adopted in the industry.[63–66] Our work extends this approach to natural rubber reinforced with carbon particles. By compounding latex, carbon particles and curing agents in an organic solvent, long chains can be retained. This division allows compounding, shaping, and curing to be optimized in separate environments, revealing opportunities to tune the microstructure and performance of carbon reinforced natural rubber beyond the limits of conventional mastication.

Long chains, once regarded as a disadvantage in processing, emerge as an advantage for performance. In particular, this work demonstrates that long chains can resolve the modulus-toughness conflict in carbon black reinforced natural rubber. It is hoped that this study informs the design of next-generation carbon black reinforced natural rubber with enhanced performance and sustainability.

10. Methods

10.1. Materials

Natural rubber latex (60 wt% rubber content) is purchased from Chemionics Corporation (OH, USA). Dicumyl peroxide (DP, 329541) and toluene (244511) are purchased from Sigma-Aldrich. Carbon black (5991R-1LBCAN, Thermal Black) is purchased from Asbury Carbons. The average particle diameter ($\sim$230) nm is provided by the supplier. All materials are used as received.

10.2. Carbon black reinforced natural rubber fabricated by toluene process

First, DP is dissolved in toluene. Then, natural rubber latex is mixed with the DP-toluene solution at a mass ratio of 1 : 6. The DP-toluene-latex mixture is stirred at 400 rpm overnight at room temperature. Separately, carbon black particles are dispersed in toluene at a mass ratio of 1 : 5. The carbon-toluene dispersion is mixed with an overhead stirrer (ONiLAB OS20-S) equipped with a dissolver blade at 1000 rpm overnight at room temperature. The resulting dispersion is then added to the DP–toluene–water–latex mixture, which is further stirred with the overhead stirrer at 1000 rpm overnight. The resulting mixture is dried in a fume hood at room temperature for four days to evaporate both toluene and water. The mass of a sample is monitored during drying and plateaus after four days. The dried, uncured compound is shaped at 90 °C for 1 hour and then cured at 140 °C for 3 hours.

In this study, the volume fractions of carbon particles are chosen as F = 0.2 and F = 0.4. The crosslink density, C, is defined as the molar ratio between DP and repeat units per polyisoprene chain. We choose $C = 10^{-3}$, 2×10^{-3}, 3×10^{-3}, 5×10^{-3}, and 10^{-2}.

10.3. Carbon black reinforced natural rubber fabricated by mastication

The dried, uncured compound is passed 100 times through a two-roll mill with a 1 mm roll gap. Then, the compound is shaped at 90 °C for 1 hour and then cured at 140 °C for 3 hours.

10.4. Scanning electron microscopy (SEM)

SEM images are taken using a Zeiss Gemini 360 FE-SEM. To prevent charging, samples are coated with 10 nm-thick Pt/Pd (80/20 composition) using a metal sputter coater (EMS 150T S, Quorum Technologies). All SEM images are taken from the cross sections of the composites.

10.5. Dynamic mechanical analysis

Strain sweep experiments are conducted using a dynamic mechanical analyzer (DMA 1, Mettler Toledo) from 0.1% to 10% strain at a constant frequency of 1 Hz and temperature of 25 °C.

10.6. Stress–stretch curves

Stress–stretch curves are measured using dogbone-shaped samples by uniaxial tension. The gauge section of each sample has a dimension of $L \times w \times t = 16 \times 2 \times 0.8$ mm, where L, w, and t are the length, width, and thickness, respectively. The stretch is defined by $\lambda = l/L$, where l is the deformed length of the sample. The nominal stress is defined by $s = P/(w \times t)$, where P is the applied force. All samples are tested under a stretch rate of 1%/s until rupture.

10.7. Strain-induced crystallization

WAXS measurements are performed using X-ray Diffraction Facility at Massachusetts Institute of Technology (Dectris Pilatus3R 300 K detector on a SAXSLAB apparatus). To reduce the background intensity fluctuation, the vacuum chamber is pumped to 0.08 mbar during the X-ray scattering measurements. Dogbone-shaped samples are stretched and then fixed to a holder. The exposure time for each test is 300 s. For each crosslink density, samples are measured at various stretches from the undeformed state to the maximum stretch. To determine the crystallinity, background contributions are subtracted. The measured 1D intensity profiles are deconvoluted into two amorphous peaks and four crystalline peaks of natural rubber, and one peak corresponding to carbon black, all fitted using Gaussian functions. In the analysis, the contribution from carbon black is decoupled. That is, crystallinity is defined by the volume fraction of rubber that crystallizes, $\chi_c = A_c/(A_c + A_A)$, where A_c is the total integrated area of the four crystalline peaks of natural rubber, and A_A is the total integrated area of the two amorphous peaks of natural rubber. The peak corresponding to carbon black is not included in the calculation. Here we follow the procedure established in the literature.[6,7,67]

10.8. Mullins effects

Each composite is loaded to increasing stretches and then unloaded in sequence. All tests are performed at a stretch rate of 1%/s. Hysteresis is defined as the ratio of the area enclosed by the loading-unloading loop to the area under the loading curve.

10.9. Pure shear tests

For each composite, we prepare two samples, with and without a notch. Both samples have the same dimension of $w \times H \times t = 50 \times 10 \times 0.8$ mm, where w, H, and t are the width, height, and thickness, respectively. For the notched sample, a long precrack of 15 mm is introduced. The stretch is defined as $\lambda = h/H$, where h is the deformed height of the sample. The nominal stress is $s = P/(w \times t)$. For the notched sample, the critical stretch where the nominal stress achieves the maximum is denoted as λ_c. Then, the strain energy per unit volume $W(\lambda_c)$ is calculated by integrating the stress–stretch curve of the unnotched sample from $\lambda = 1$ to $\lambda = \lambda_c$. The toughness is calculated as $G_c = H \times W(\lambda_c)$. All tests are performed at a stretch rate of 1%/s.

Conflicts of interest

There are no conflicts to declare.

Data availability

The data that support the findings of this study are available from the corresponding author upon reasonable request.

Acknowledgements

This work is supported by the National Science Foundation under MRSEC (DMR-2011754). Z. S. acknowledges the support of the Air Force Office of Scientific Research under award number FA9550-20-1-0397. M. W. M. Tan gratefully acknowledges the financial support under the College of Engineering (CoE) International Postdoctoral Fellowship (IPF), which is jointly provided by the Ministry of Education, Singapore, and Nanyang Technological University, Singapore.

References

1 B. Westall, *Polymer*, 1968, **9**, 243–248.
2 N. Hayeemasae, S. Soontaranon and A. Masa, *Prog. Rubber Plast. Recycl. Technol.*, 2025, **41**, 36–52.
3 L. R. G. Treloar, *The Physics of Rubber Elasticity*, Oxford University Press, Oxford, 1975.
4 Y. Tanaka and L. Tarachiwin, *Rubber Chem. Technol.*, 2009, **82**, 283–314.
5 M. Tosaka, S. Kohjiya, S. Murakami, S. Poompradub, Y. Ikeda, S. Toki, I. Sics and B. S. Hsiao, *Rubber Chem. Technol.*, 2004, **77**, 711–723.
6 L. Kong, J. Zhang, S. Huang, R. Zhang, J. Li, Z. Xie and J. Wu, *Macromolecules*, 2025, **58**, 3109–3118.
7 G. Nian, Z. Chen, X. Bao, M. W. M. Tan, Y. Kutsovsky and Z. Suo, *Nat. Sustainability*, 2025, **8**, 692–701.
8 H. P. Zhang, J. Niemczura, G. Dennis, K. Ravi-Chandar and M. Marder, *Phys. Rev. Lett.*, 2009, **102**, 245503.
9 S. Kohjiya and Y. Ikeda, *Chemistry, Manufacture and Applications of Natural Rubber*, Woodhead Publishing, Cambridge, UK, 2021.
10 E. E. Ehabe, G. E. Nkeng, A. Collet and F. Bonfils, *J. Appl. Polym. Sci.*, 2009, **113**, 2785–2790.
11 D. J. Harmon and H. L. Jacobs, *J. Appl. Polym. Sci.*, 1966, **10**, 253–257.
12 Y. Zhou, W. Zhang, J. Hu, J. Tang, C. Jin, Z. Suo and T. Lu, *J. Appl. Mech.*, 2020, **87**, 031002.
13 A. K. Bhowmick, *J. Mater. Sci.*, 1986, **21**, 3927–3932.
14 M. Nasir and G. K. Teh, *Eur. Polym. J.*, 1988, **24**, 733–736.
15 C. M. Kok and V. H. Yee, *Eur. Polym. J.*, 1986, **22**, 341–345.
16 A. K. Bhowmick, *Polym. Rev.*, 1988, **28**, 339–370.
17 M. Rubinstein and R. H. Colby, *Polymer Physics*, Oxford University Press, Oxford, 2003.
18 X. Bao, G. Nian, Y. Kutsovsky, J. Kim, Q. Jiao and Z. Suo, *Soft Matter*, 2023, **19**, 5956–5966.
19 J. Kim, G. Zhang, M. Shi and Z. Suo, *Science*, 2021, **374**, 212–216.
20 G. Nian, J. Kim, X. Bao and Z. Suo, *Adv. Mater.*, 2022, **34**, 2206577.
21 J. Steck, J. Kim, Y. Kutsovsky and Z. Suo, *Nature*, 2023, **624**, 303–308.
22 M. W. M. Tan, G. Nian, Z. Chen, X. Bao, Y. Kutsovsky and Z. Suo, *Proc. Natl. Acad. Sci. U.S.A.*, 2025, in press.

23 Y. Fan, G. D. Fowler and M. Zhao, *J. Cleaner Prod.*, 2020, **247**, 119115.
24 J.-B. Donnet, *Carbon Black: Science and Technology*, CRC Press, Boca Raton, FL, 1993.
25 H. Zhang, A. K. Scholz, J. de Crevoisier, D. Berghezan, T. Narayanan, E. J. Kramer and C. Creton, *J. Polym. Sci., Part B: Polym. Phys.*, 2015, **53**, 422–429.
26 M. J. Wang, C. A. Gray, S. A. Reznek, K. Mahmud and Y. Kutsovsky, *Kirk-Othmer Encycl. Chem. Technol.*, 2003, **4**, 761–803.
27 T. Witten, M. Rubinstein and R. Colby, *J. Phys. II*, 1993, **3**, 367–383.
28 C. G. Robertson and N. J. Hardman, *Polymers*, 2021, **13**, 538.
29 P. B. Stickney and R. D. Falb, *Rubber Chem. Technol.*, 1964, **37**, 1299–1340.
30 T. Spratte, J. Plagge, M. Wunde and M. Klüppel, *Polymer*, 2017, **115**, 12–20.
31 J.-M. Chenal, C. Gauthier, L. Chazeau, L. Guy and Y. Bomal, *Polymer*, 2007, **48**, 6893–6901.
32 Q. Demassieux, D. Berghezan, S. Cantournet, H. Proudhon and C. Creton, *J. Polym. Sci., Part B: Polym. Phys.*, 2019, **57**, 780–793.
33 J. Chen, M. Hu, Y. Li, R. Li and L. Qing, *Polymers*, 2023, **15**, 2051.
34 M. Qu, F. Deng, S. M. Kalkhoran, A. Gouldstone, A. Robisson and K. J. Van Vliet, *Soft Matter*, 2011, **7**, 1066–1077.
35 H. Zhang, A. K. Scholz, J. De Crevoisier, F. Vion-Loisel, G. Besnard, A. Hexemer, H. R. Brown, E. J. Kramer and C. Creton, *Macromolecules*, 2012, **45**, 1529–1543.
36 J. E. Mark, B. Erman and M. Roland, *Science and Technology of Rubber*, Academic Press, San Diego, CA, 1994.
37 M. Morton, *Rubber Technology*, Springer Science & Business Media, Dordrecht, 2013.
38 T. Gao, R. Xie, L. Zhang, H. Gui and M. Huang, *Int. J. Polym. Sci.*, 2015, **2015**, 1–6.
39 M. D. Rintoul and S. Torquato, *J. Phys. A: Math. Gen.*, 1997, **30**, L585.
40 L. Karasek, B. Meissner, S. Asai and M. Sumita, *Polym. J.*, 1996, **28**, 121–126.
41 S. Torquato, *Random heterogeneous materials: microstructure and macroscopic properties*, Springer, 2002.
42 M. Rubinstein and S. Panyukov, *Macromolecules*, 2002, **35**, 6670–6686.
43 L. J. Fetters, D. J. Lohse, D. Richter, T. A. Witten and A. Zirkel, *Macromolecules*, 1994, **27**, 4639–4647.
44 P. J. Flory, *Principles of Polymer Chemistry*, Cornell University Press, New York, 1953.
45 A. N. Gent and B. Park, *J. Mater. Sci.*, 1984, **19**, 1947–1956.
46 R. F. Gibson, *Principles of composite material mechanics*, CRC press, 2007.
47 E. Guth, *J. Appl. Phys.*, 1945, **16**, 20–25.
48 G. Heinrich and M. Klüppel, *Adv. Polm. Sci.*, 2002, **160**, 1–44.
49 J.-M. Chenal, L. Chazeau, L. Guy, Y. Bomal and C. Gauthier, *Polymer*, 2007, **48**, 1042–1046.
50 B. Huneau, *Rubber Chem. Technol.*, 2011, **84**, 425–452.
51 S. Poompradub, M. Tosaka, S. Kohjiya, Y. Ikeda, S. Toki, I. Sics and B. S. Hsiao, *J. Appl. Phys.*, 2005, **97**, 103529.
52 K. Sengloyluan, K. Sahakaro, W. K. Dierkes and J. W. M. Noordermeer, *eXPRESS Polym. Lett.*, 2017, **11**, 1003–1022.
53 K. Katueangngan, T. Tulyapitak, A. Saetung, S. Soontaranon and N. Nithi-Uthai, *J. Vinyl Addit. Technol.*, 2020, **26**, 291–303.
54 W. Borapak, N. Chueangchayaphan, S. Pichaiyut and W. Chueangchayaphan, *J. Appl. Polym. Sci.*, 2020, **137**, 48738.
55 C. Chen, Z. Wang and Z. Suo, *Extreme Mech. Lett.*, 2017, **10**, 50–57.
56 J. Steck, C. H. Ahn and Z. Suo, *Annu. Rev. Mater. Res.*, 2025, **55**, 333–358.
57 V. Tvergaard and J. W. Hutchinson, *J. Mech. Phys. Solids*, 1992, **40**, 1377–1397.
58 A. G. Evans, *J. Am. Ceram. Soc.*, 1990, **73**, 187–206.
59 W. L. Cox and C. R. Parks, *Rubber Chem. Technol.*, 1966, **39**, 785–797.
60 L. C. Yanyo, *Int. J. Fract.*, 1989, **39**, 103–110.
61 H. Peidayesh, Z. Nógellová and I. Chodák, *Materials*, 2023, **17**, 71.
62 J. Kruželák, R. Sýkora and I. Hudec, *Chem. Pap.*, 2016, **70**, 1533–1555.
63 Q. Zhao, F. Niu, J. Liu and H. Yin, *Polymers*, 2024, **16**, 1899.
64 Y. Sui, Q. Lai, W. Nie, S. Tang, C. Wang and H. Bian, *J. Appl. Polym. Sci.*, 2022, **139**, e52971.
65 M. Wang, J. Song and D. Dai, *Continuous manufacturing process for rubber masterbatch and rubber masterbatch prepared therefrom*, *US Pat.*, US9758627B2, 2017.
66 Z.-R. Chen, S. Araki, W. M. Cole, W. Hergenrother and S. Warren, *Solution masterbatch process using fine particle silica for low hysteresis rubber*, *US Pat.*, US7312271B2, 2007.
67 S. Beurrot-Borgarino, B. Huneau, E. Verron and P. Rublon, *Int. J. Fatigue*, 2013, **47**, 1–7.